International Journal of Communication and Information Technology

Kadiri Kamoru
The Federal Polytechnic Offa Kwara State and the Polytechnic Iresi Osun State, Nigeria

Keshinro Kazeem Kolawole
Department of Computer Engineering, LASPOTECH, Ikorodu, Lagos, Nigeria

Omotayo Mayowa
Department of Electrical and Electronic Engineering, Osun State Polytechnic Iree, Osun State, Nigeria

Enem Theophilus
Department of Cybersecurity, Air Force Institute of Technology, Nigerian Air Force Base, Kaduna, Nigeria

Development of rain attenuation prediction in south west Nigeria on terrestrial link using artificial neural Network

Kadiri Kamoru, Keshinro Kazeem Kolawole, Omotayo Mayowa and Enem Theophilus

Abstract
The predicted precipitation accuracy in light of the current global climate change is very important. The Back-Propagation Neural Network (BPNN) technique then utilized the Artificial Neural Network (ANN) to correctly forecast rainfall. The study is based on data from three Nigerian terrestrial microwave connections operating at frequencies of 23 and 38 GHz. At 23 GHz, a normal distribution with an average of zero is the best represented fade slope distribution, contrary to the model ITU-R earth to satellite rain fade slope. Based on the data analysis observed at 23 GHz, a novel prediction model is developed. The suggested model is validated using 38 GHz fade slope data and shown to work well with nearly all attenuation levels. A chi-square fitness test is used to further validate the model. The suggested model will be critical in the development of rainfall mitigation methods for tropical terrestrial connections. The findings of the research indicate that BPNN models may be utilized as a prediction algorithm that offers a high predictive accuracy of three types of design: 500, 1000 and 1,500.The experiment examined data on precipitation using the BPNN Architecture's two-hidden layers, from three periods of time [2-50-10-1, 500]. The average square error is used for categorization work performance evaluation. The results of the experiment indicate that the design of the 100-year-old [2-50-20-1, MSE of 0 00096341] is excellent. Moreover, the BPNN algorithm provides an efficient Southwestern Nigeria predictor model.

Keywords: Artificial neural network (ANN), prediction, rain attenuation and terrestrial link

1. Introduction
The high bandwidth and low traffic congestion are typical in today's microwave point-to-point networks with frequencies over 10 GHz [1]. However, rain attenuation dominates the performance of the fixed service (FS) in these frequency bands. Pluvial diminution losses are compounded by rainfall inhomogeneity, which further increases the impact on link performance of propagation effects (ITU-R) [2, 4]. A severe issue may develop, particularly when rain attenuation is high in low percentages of time. For decades, the International Telecommunications Union-Radio Sector (ITU-R) has been looking for a worldwide model to forecast rain-inducing attenuation at terrestrial microwave connections [5, 6]. Tropical and equatorial radio connections utilizing the ITU-R forecast technique for rain attenuation provide unsatisfactory results. The most significant amount for determining the rain attenuation for terrestrial and slant roads per unit distance (dB/km) is the rain attenuation. Specific attenuation is an essential component in developing a prediction rain attenuation model that minimizes the effect on a Satellite dish and enables direct light measurements to be compared to model forecasts, [7, 12]. As a solution, the Ku-band (11/14 GHz) is proposed. As a result of rain, the radio wave is expected to be attenuated significantly. When it comes to countries with tropical rainfall climates, using Ku/ka-band is more complicated than when it comes to countries with temperate climates. For countries with temperate climates, the accuracy of the present rainfall prediction models will be tested [10]. As a result of these effects, extreme flooding and droughts have been reported. As a result, a good and accurate rain-prediction method is essential for predicting the effects.

As a consequence, many techniques were created to provide effective and reliable results for rainfall and weather forecasting. The predictions of rainfall were produced using a statistical model. Examples of models that operate with the decrease in the data equation include a simple regression analysis (SRA), decomposition, exponential smoothing (ES) (ARIMA).

Corresponding Author:
Kadiri Kamoru
The Federal Polytechnic Offa Kwara State and the Polytechnic Iresi Osun State

The non-linear nature of weather data has been shown in a number of studies to make these methods of forecasting rainfall and weather still inaccurate. It is true that the statistical method of rainfall prediction is sometimes successful in producing accurate predictions [6, 10, 11].

In spite of the various globally accepted rain attenuated models developed for optimal link planning especially for communications in the Ku band, digital terrestrial television links still suffer noticeable impairments during heavy rainfall events this accounting for total loss of the signal. The issue of frequency scaling is not simple, since atmospheric gases and clouds have a significant attenuation impact above 20GHz. Consequently, the physical components of attenuation must be separated. Attenuation components are then scaled using particular scaling factors derived from ground meteorological data. The contribution of frequency scaling to the total uplink prediction error is higher than that of downlink prediction, according to an analysis of the contributions.

2. Materials and Methods
A. Site Details
Due to its sea exposure, the tropical climate of Nigeria is marked by constant temperatures, high humidity and substantial annual average precipitation of 4184.3mm. Thunderstorm precipitation is the most common type of precipitation in Nigerian climes. Annual moon-soon cycles (from October to March north-east, from April to September south-west) have an effect on the distribution of the monthly rainfall based on per minute. Table 1 provides information on the measurement locations.

Table 1: Measurement sites' details

Location	Longitude (^0E)	Latitude (^0N)	Frequency (GHz)	Pathlength (km)
Ibadan	4.01	7.21	14.8	11.3
Osogbo	4.31	7.42	14.8	5.83
Akure	5.12	7.18	15.3	4.85
Abeokuta	3.21	7.07	14.8	3.96
Ilorin	4.34	8.32	14.8	3.48
Ikeja	6.25	6.25	14.8	5.36

Source: National Space Research and Development Agency (NASRDA, 2021)

B. Procedure of the experiment
It was gathered from Nigerian space research agency Abuja. A related data collecting and processing system exists as part of any microwave system. With every second of the data gathered, each link runs at a frequency of 23 GHz and 38 GHz. For both broadcast and receive antennas, horizontal polarization is utilized (for example, the elevation angle is approximately zero degrees). Rain attenuation tests were performed utilizing radome-covered antennas, to guarantee reliable results. The antennas were positioned to prevent the sidelobes from facing the ground. Sidelobe contamination (noise) is thus maintained to a minimum. Additional variables like scintillation and air absorption along the propagation path were not taken into consideration in the study. With the conversion conversation from manufacturers, the AGC level (volt) automatic gain control was transferred to the matching receiver data in dBm. The conversion process is unsteady, with fluctuations of almost ±4dB. Rain attenuation data based on the calibration is 98 percent correct. The highest signal strength is approximately

50 dB with significant attenuation in the dynamic range (i.e., rain).

Table 2: 15GHZ Link specifications

Type of antenna	Front-fed parabolic
Frequency band (GHz)	23 GHz, 38 GHz
Polarization	Horizontal
Maximum transmit power (dBm)	+18.0
10^{-6} BER (2X2 Mbps) Received threshold (dBm)	-84.0
Antenna beam width	2.3^0
Dynamic range (dB)	50 Db
Antenna for both transmit and receive side	Size (m) 0.6 Gain (dBi) 37.0

The rainfall measurements were collected concurrently by placing a Casella rain gauge equipped with a programmed data recorder fairly near to the receiving antenna. The rain gauge is of the kind of tipper and the size of the bucket is 0.5 mm. The tipping time cannot be recorded, but the number of tips has been captured and saved in the built-in rain gauge data recorder. The sensitivity and availability of the rain gauge are 0.5mm/min and 100%, respectively. The temperature range is −10 to 500C and extremely dependable with ±1.00 percent tipping accuracy

A Casella rain gauge with a programmed data recorder was positioned very close to the receiving antenna in order to capture the rain rate. Tipping 0.5mm rain bucket gauge is utilized. The tipping time was not recorded; however, the number of tips was recorded. The rain gauge is set at 0.5 mm/min and 100% in terms of sensitivity and availability. Operating temperature range 10 to 500C; 1.00% precision of tipping.

Rainfall measurements were performed over a four-year period in Ibadan, Osogbo, Akure, Abeokuta, Ilorin and Ikeja. The rainfall rates were collected at six locations with an integrated time of one minute, and the average measurement values for four years were associated with the one-year attenuation data measured. Data from the Nigerian Meteorological Station (NMS) were used for the other four sites (Ibadan, Ilorin, Akure and Ikeja). The Chebil and Rahman model is thus utilized to convert 1-hour rain data into 1-minute rain data.

3. Prediction of Rain Rate on per minute with both Forward and Backward Neural Network
For the 500 input weights, there are only a limited amount of training values accessible. In order to make the network smaller, it was essential to do so. Given the interconnectedness and intricacy of the network's internal connections, it is not always clear which input parameters are essential and whether any of them should be discarded. Even simple techniques, such as comparing runs with various input combinations omitted, may provide findings that are difficult to understand. "Network pruning" is a more robust approach. An extra criteria of weight minimization is used when the network is pruned. This is achieved by using an algorithm that takes into consideration Size as well as number of weights in a complexity term Z.

$$Z = \sum_{i=1}^{N_1} \sum_{j=1}^{N_2} \left(\frac{w_{1ij}^2/w_0^2}{1+w_{1ij}^2/w_0^2} \right), \qquad (1)$$

Where W_{1ij} are the input and the second layer connected

weights; where W_0 is the experimentally obtained weight scaling parameter; Where input and second-layer nodes areN1 and N2.

The total cost function of the improved network is decreased

$$C = msd + Z. \tag{2}$$

The learning technique adjusts the weight to the gradient of the total cost function C with the low complexity network constraints. Unnecessary nodes are weighed down. Small input weight factors may be eliminated. To validate this pruning method, a random number input was supplied to the ANN. We verified that weights linked to this input have been pruned to zero.

When CCD data at many different temperature thresholds were incorporated, the raw TIR data and associated geographic variation could be removed. It was also determined that latitude and longitude, which indicate a station's location, were not significant. As detailed in the next section, improvements in validation statistics corroborated these findings. Thirty input variables and two hidden levels of the settings generated better validation statistics than the one of the input variables with 30 and two hidden layers

The effect of network training on a variety of stations has also been evaluated. Maximum results were achieved during the training using all 25 pixels of the calibration gauge, but results with just two of them may be obtained.

A minor issue with this ANN setup was that zero rainfall was difficult to produce. This led to estimations of extremely little precipitation (< 1 mm) across vast regions. Although this is not substantial on a daily basis, it is clearly non-physical and may create issues if daily values are included over longer periods. All pixel estimations should be set to nil for CCD = 0 for Tt = -300C.

Due to the architecture of the ANN, zero precipitation could not be produced. This resulted in estimates of extremely little precipitation (<1 mm) across vast regions. When daily data are mixed over longer periods, this may create problems. If CCD = 0 for Tt = -300C, the estimations of pixels were set to nil.

For the remainder of this finding, the final technique stated in the previous paragraphs will be used by TAMANN.

3.1 BPNN Flow for Prediction
These are the steps of the BPNN algorithm for predicting precipitation data:
1. all weights begin simultaneously;
2. Repeat steps 2-8 if the termination condition has not been fulfilled;
3. Then repeat steps 3-8 for each data set

Phase 1: Future spread of feed
iv. The signals are received and sent to the top unit concealed from view by each unit. Calculate all output on hidden units of layer z_j (j = 1, 2, …, p)

Determine the output of the network output. y_k (k = 1, 2, m)

$$y\_net_k = w_{ko} + \sum_{j=1}^{p} z_j w_{kj}; y_k = f(y\_net_k) = \frac{1}{1+e^{-y\_net_k}} \tag{3}$$

Phase 2: Back to Future
1. Factor = output unit calculation based on unit output

inaccuracy y_k (k = 1, 2, …, m)
1.

$$\delta_k = (t_k - y_k) \, f'(y\text{-}net_k) = (t_k - y_k) \, y_k(1-y_k) \tag{4}$$

t_k = output target; δ = output unit that will be used in the layer underneath the weight change

Calculate weight change w_{kj}, with the learning rate $\alpha(\delta w_{ji} = \alpha \delta_k z_j$, k = 1,2,…,m; j = 0,1,…,p)

Calculate the hidden layer factor δunit based on inaccuracy on each unit of hidden layer z_j (j = 1, 2, …, p)

$$\delta\_net_j = \sum_{k=1}^{m} \delta_k w_{kj} \tag{5}$$

Factor δ hidden layer unit [$\delta_j = \delta\_netj \, f'(z\_net_j) = \delta\_netj \, zj(1-z_j)$]

Calculate weight change rate v_{ji} [$\delta v_{ji} = \alpha \delta_k z_j$, k = 1,2,…,p; j = 0,1,…,n]

Phase 3: Weight modification
Calculate the weight of all the changes that led to the output unit

$$wk_{j(new)} = wk_{j(old)} + \delta_{wji}; (k = 1, 2, …, p; j = 0, 1, …, n) \tag{6}$$

Weight changes that led to the hidden layer units

[$v_{kj(new)} = v_{kj(old)} + \delta_{vji}$; (j = 1,2,…,p; w = 0,1,…,n)

Inputs	First	Second	Output
Layer	Hidden	Hidden	Layer
(2)	Layer	Layer	(1)
	(50)	(20)	

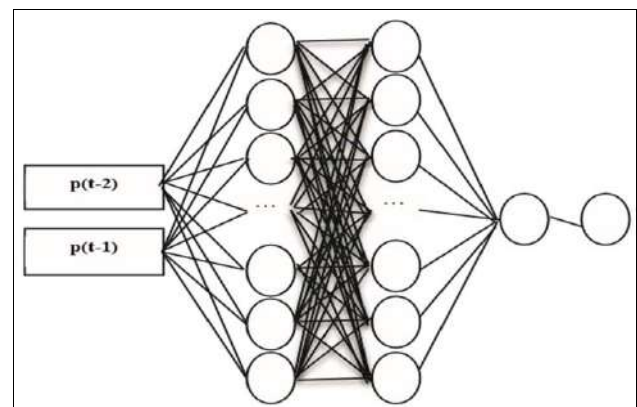**Fig 1:** BPNN architecture

P = [p(t-2), p(t-1)] and the output layer were chosen in Table 3. for T-2, t-1, and T for all the input layers of this research. Two layers were used for illustration of the hidden layers: the first layer was 50 pixels thick and the second layer was 10 pixels thick. As Figure 1 shows, there are numerous components of the BPNN.

4. Result and Discussion
4.1 Comparison with other Rain Attenuation Models
This study compares the findings of slant trajectory measurements with the two generally recognized models (IITU-R model P.618-10 and Crane global model). The emphasis is on attenuation induced by rain. As demonstrated

in Figure 2, when both models have understated the rainfall rate observed, particularly in high rates, rainfall exceeding 4-year measures was comparable to the ones anticipated by ITU-R P.837-6 and the Crane global model. For example, the first forecasts that the rain rate is 0.01 percent, while it is 90.2 mm/h, and the second predicts the rain rate is 90.2 mm/h. The measured rain attenuation observed is compared with forecasts, as illustrated in Figure 3 and then tested using the ITU-R P.311-13 for the two prediction models.
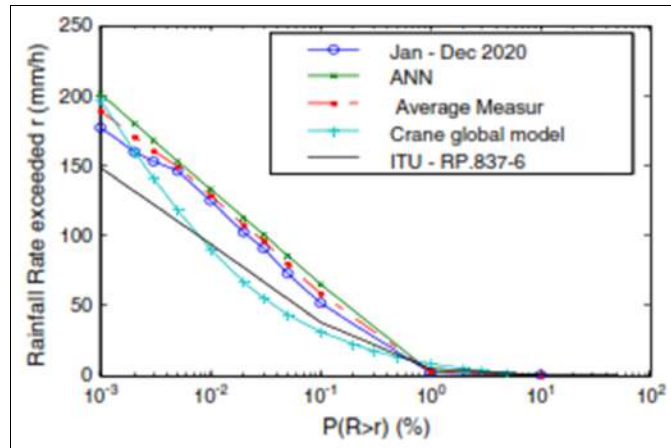

Fig 2: Comparison of rainfall rate exceedance.
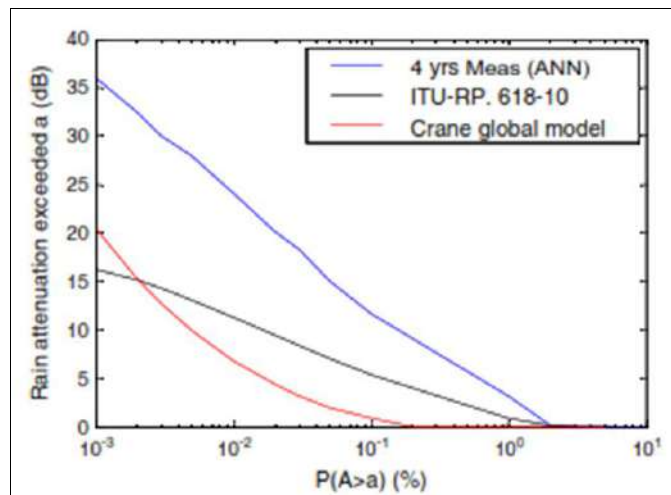

Fig 3: Comparison of rain Attenuation Exceedance.

The fading slope's conditional distribution functions for the 1, 3, 5, 8, 10 and 15 dB attenuation levels at 23 GHz are shown on one graph in Fig. 3. The following observations are taken into account. In the first place, all the fading pitch distributions presented are symmetric to 0 dB/s. Second, all CPDFs follow the usual zero average distribution. Third, as the attenuation level rises, the dispersion gets wider. Finally, with the reduction level, the amplitude of the fading slope rises, while the quantity of data drops. The T-test is used to demonstrate that the fading slope distribution follows the normal distribution. For the T-test, two hypotheses are examined. The first is the null hypothesis (H = 0), which assumes that the observed data follow a standard distribution of μ = 0. The second is the alternative (H = 1) hypothesis, wherein the observed data are taken into account, follow a normal distribution of mean μ to 0.

$$t = \frac{\bar{x} - \mu}{\sigma/\sqrt{n}}$$

`   (7)

where $\bar{x}$, σ are the mean and default deviation of the data examined. The data size is denoted by n. Table 3 sums up the findings of the test and demonstrates that the T test passes with a meaning level of 0.05 for all attenuation levels at 23 GHz. This implies that the null hypothesis is accepted with 95% confidence.

Table 3: T-test results for the 23 GHz connection measured data

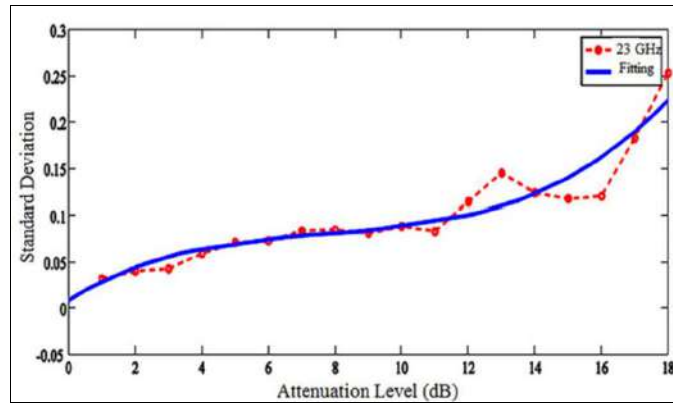| Attenuation level (dB)	N	H
1	G8 938	0
2	51 526	0
3	34 127	0
5	7819	0
8	1928	0
10	569	0
15	85	0

Fig 4: Comparison between the standard deviation predicted and measured depending on 23 GHz attenuation levels.

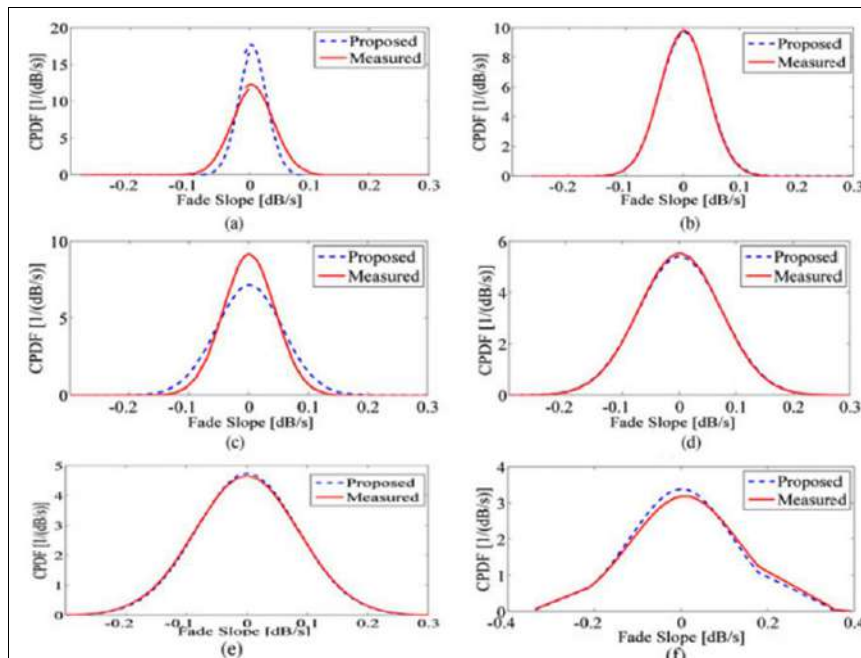**Optimization with Adaptive neuro-fuzzy inference systems (ANFIS)**

Fig 5: Comparison of the observed data at 23 GHz for fade slopes for attenuation level (a) 1 dB; 2 dB; (c) 3 dB; (d) 5 dB; (e) 8 dB; and (f)
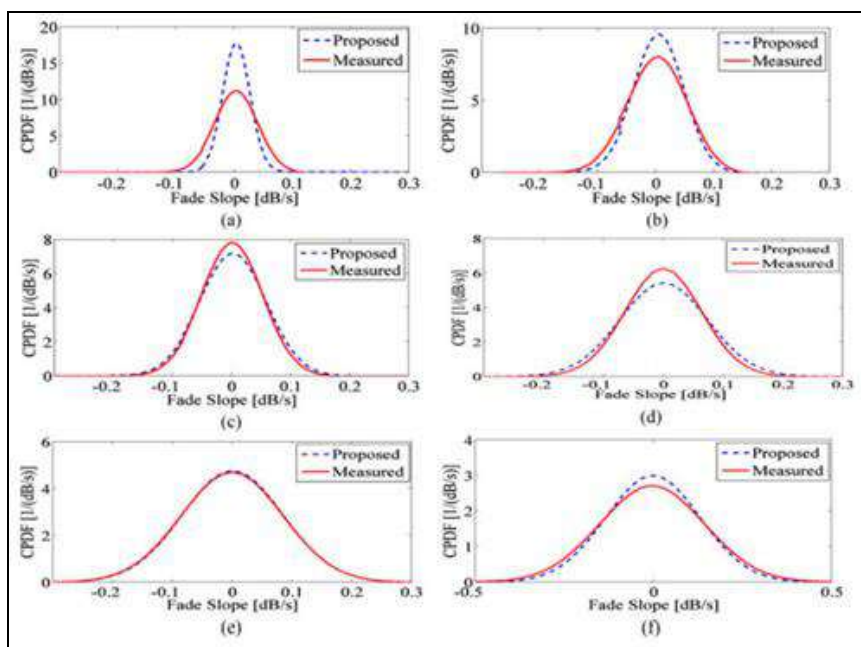

Fig 6: CPDF of fading slopes of the proposed model and observed data at 38 GHz for (a) 1 dB mitigation; (b) 2 dB; (c) 3 dB; (d) 5 dB; (e) 8 dB; and (f) 15 Db

Table 4: The calculated (χ^2_{comp}) and theoretical (χ^2_{th}) χ2 values of 0.05 for the three experimental connections are shown in the same degree of freedom (df)

Attenuation level (dB)	23GHz			38GHz		
	d_f	χ^2_{comp}	χ^2_{th}	d_f	χ^2_{comp}	χ^2_{th}
1	68 938	75 781	69 550	35 716	64 289	36 157
2	51 526	67	52 055	29 508	1427	29 909
3	34 127	9759	34 558	41 890	1427	42 367
5	7819	8	8026	19 982	1476	20 312
8	1928	2	2031	6816	4	7009
15	85	2	108	1135	16	1214

$$p(\xi|A) = \frac{1}{\sigma_\xi \sqrt{2\pi}} exp\left(0.5\left(\frac{\xi - \mu}{\sigma_\xi}\right)^2\right) \tag{8}$$

In this equation, the standard deviation is the sole parameter that affects the distribution. Figure 4. shows the standard deviation for that metric in relation to the attenuation levels measured at 23 GHz. MATLAB fitting tools may be used to determine the optimum fit

$$\sigma_\xi = 0.00012A^3 - 0.003A^2 + 0.027A - 0.0016 \tag{9}$$

The correct fit is shown by the (12) curve in Figure 4. Since the average is zero, (11) may be read as

$$p(\xi|A) = \frac{1}{\sigma_\xi \sqrt{2\pi}} exp\left(0.5\left(\frac{\xi}{\sigma_\xi}\right)^2\right) \tag{10}$$

The prior study's equations (4.9) and (4.10) may be utilised to create a new model for predicting the fading pitch distribution. To assess their performance, Figure 4. shows plots of both the CPDF of the proposed model's fading slopes and actual data of various attenuation levels at 23 GHz. At all attenuation levels except 1 and 3 dB, the new model effectively fits the observed data. However, when comparing the results in Figures 4. And 5, the new model's predicted distribution outperforms the 3 dB ITU-R distribution. It may be assumed that the new model will outperform the ITU-R model for any attenuation level greater than 2 dB
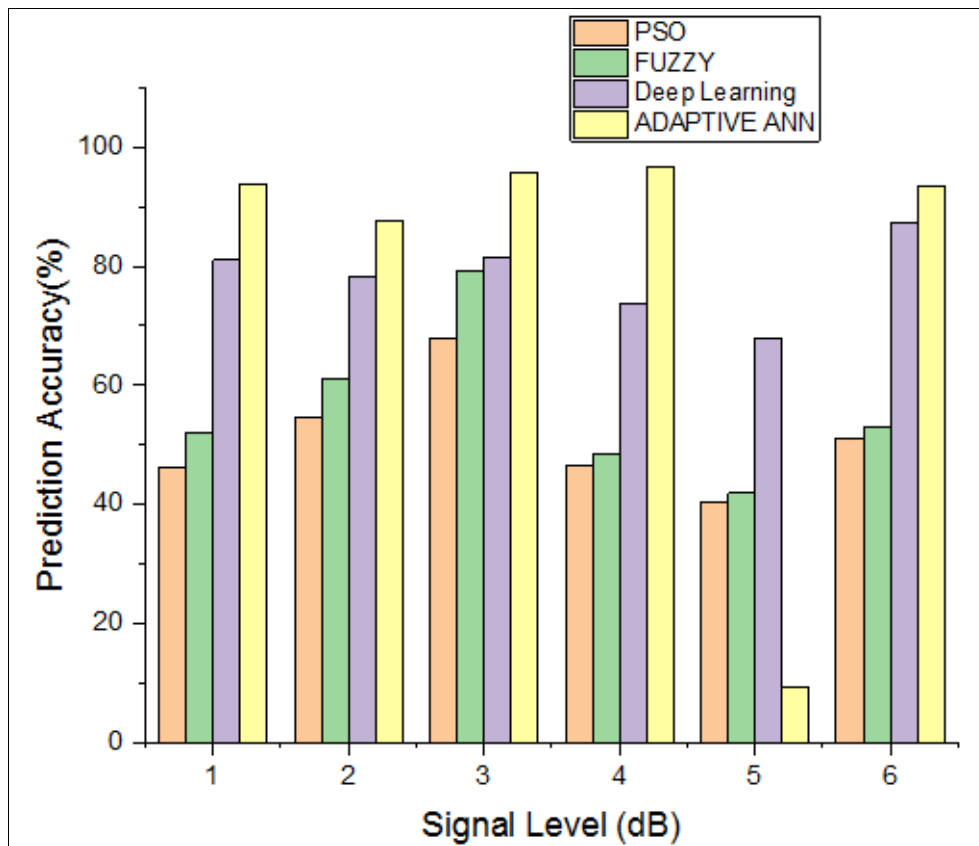

Fig 7: Comparison with other Empirical Methods

Fig 7 shows the comparison with other existing method based on the prediction accuracy. Adaptive ANN shows the best result when compared to PSO, FUZZY and DEEP Learning. Adaptive ANN shows best accuracy at each signal level.

5. Conclusion
In this study the most recent and renowned comprehensive evaluation of rain attenuation models for the terrestrial connection was carried out. The existing models are classified as physical, statistical, empirical, optimization and

pitch models depending on the design and wording. We evaluated innovative concepts, input parameters, advantages and disadvantages. A thorough assessment was given and assessed of the rain attenuation model of different terrestrial connections. According to this research, no prediction model can be seen as a worldwide model to meet all the criteria for a wide range of infrastructure features, geographical areas or climatic change throughout the period.

6. Reference

1. AO Ayo, Owolawi PA, Ojo JS, Mpoporo LJ. Rain Impairment Model for Satellite Communication Link Design in South Africa using Neural Network, 2020. Doi: 10.1109/IMITEC50163.2020.9334080.
2. Livieratos SN, Cottis PG. Rain attenuation along terrestrial millimeter wave links: A new prediction method based on supervised machine learning, IEEE Access, 2019, 7. Doi: 10.1109/ACCESS.2019.2939498.
3. Ojo JS, Owolawi PA. Characterization of rain heights due to 0° isotherm in tropical and subtropical climates: implication on rain-induced attenuation prediction, Theor. Appl. Climatol. 2019;135:1-2. Doi: 10.1007/s00704-018-2382-z.
4. Polz J, Chwala C, Graf M, Kunstmann H. Rain event detection in commercial microwave link attenuation data using convolutional neural networks, Atmos. Meas. Tech. 2020;13:7. Doi: 10.5194/amt-13-3835-2020.
5. Obiyemi OO, Ibiyemi TS, Ojo JS. On validation of the rain climatic zone designations for Nigeria, Theor. Appl. Climatol. 2017;129:1-2. Doi: 10.1007/s00704-016-1787-9.
6. Shaker FK, Ali MAA. Multi-Beam Free-Space Optical Link to Mitigation of Rain Attenuation, J. Opt. Commun. 2021;42:2. doi: 10.1515/joc-2018-0015.
7. Orellana-Alvear J, Célleri R, Rollenbeck R, Muñoz PP, Contreras, Bendix J. Assessment of native radar reflectivity and radar rainfall estimates for discharge forecasting in mountain catchments with a random forest model, Remote Sens.2020;12:12. Doi: 10.3390/rs12121986.
8. Habi HV, Messer H. Recurrent Neural Network for Rain Estimation Using Commercial Microwave Links, IEEE Trans. Geosci. Remote Sens. 2021;59:5. Doi: 10.1109/TGRS.2020.3010305.
9. P Hema Sekhar, Dr. Kesavulu Poola, K Raja Sekhar, Dr. M Bhupathi Naidu. Modelling and prediction of coastal Andhra rainfall using ARIMA and ANN models. Int J Stat Appl Math. 2020;5(6):104-110.
10. Han C, Duan S. Impact of atmospheric parameters on the propagated signal power of millimeter-wave bands based on real measurement data, IEEE Access.2019, 7. Doi: 10.1109/ACCESS.2019.2933025.
11. Xian M, Liu X, Yin M, Song K, Zhao S, Gao T. Rainfall Monitoring Based on Machine Learning by Earth-Space Link in the Ku Band, IEEE J. Sel. Top. Appl. Earth Obs. Remote Sens. 2020, 13. Doi: 10.1109/JSTARS.2020.3004375.
12. Diba FD, Samad MA, Choi DY. The Effects of Rain on Terrestrial Links at K, Ka and E-Bands in South Korea: Based on Supervised Learning, IEEE Access, 2021, 9. Doi: 10.1109/ACCESS.2021.3049825.